SFB 823

Discussion Paper
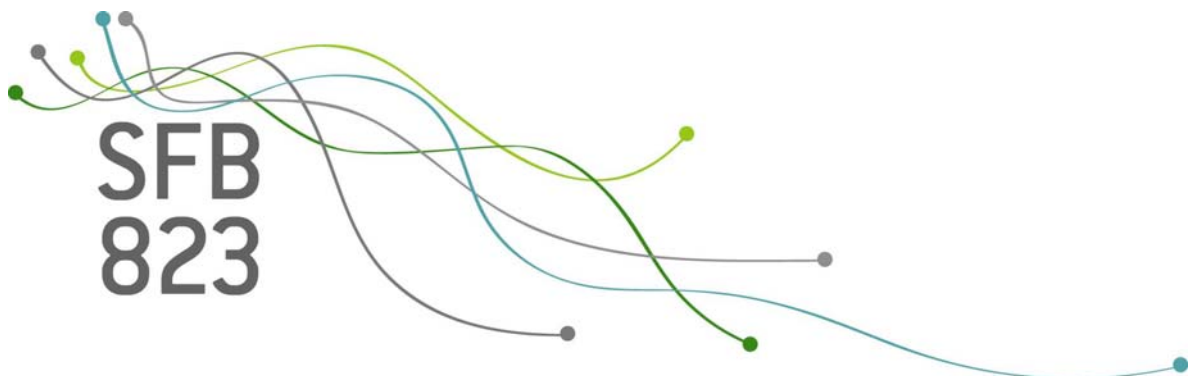
Prediction of in-flight particle properties in thermal spraying with additive day-effects

André Rehage, Nikolaus Rudak, Birger Hussong, Sonja Kuhnt, Wolfgang Tillmann

Nr. 6/2012

SFB 823

Technische Universität Dortmund

SFB 823, B1

Prediction of in-flight particle properties in thermal spraying with additive day-effects

André Rehage, Nikolaus Rudak, Birger Hussong,

Sonja Kuhnt, Wolfgang Tillmann

February 7, 2012

Contents

1. Introduction

Thermal spraying technology can be employed to apply a particle coating on a surface, e.g. for wear protection or durable medical instruments. Due to uncontrollable day-effects thermal spraying processes are lacking in reproducibility. This fact, combined with a time-consuming and not immediately available analysis of the quality of the coating, leads us to measure and use in-flight properties of the particles. Figure 1.1 shows the considered set-up of the process.
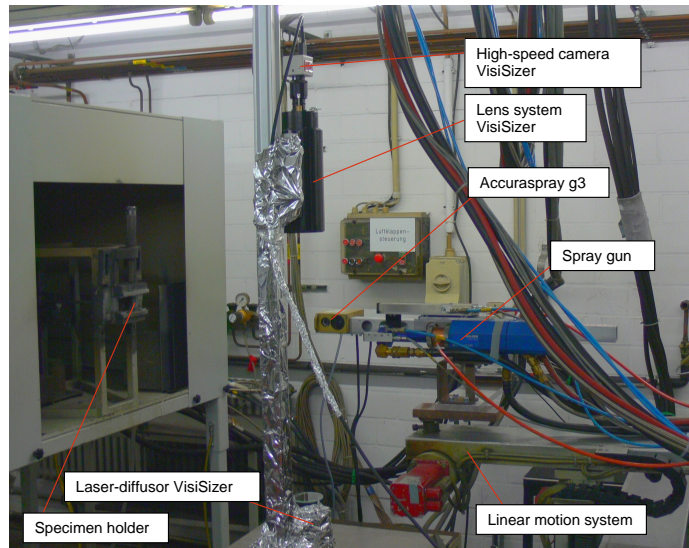

Figure 1.1: Measuring in-flight particles in a thermal spraying process

In this contribution we focus on the relationship between process parameters and properties of the particles in-flight. We aim at a strategy which allows us to predict particle properties based on prediction models from an initial full experiment together with only few experiments on the day of prediction. Preceding screening experiments (Tillmann *et al.*, 2010) identified kerosine level, stand-off-distance, feeder disc velocity and Lambda, which is defined as a kind of the kerosine/oxygen ratio, as parameters to influence in-flight properties. As a next step HVOF spraying experiments have been conducted with input parameters varied by a central-composite design. In a first approach to the complex prediction problem we fit individual prediction models to the measured in-flight properties temperature, velocity, flame intensity and flame width. Suitable statistical models are provided by the class

3

of generalized linear models (GLM). A previous analysis of similar data showed that normal and gamma distributions as well as different link functions should be considered (Hoyden, 2011). The fitted models constitute the basis for day-adjusted prediction models, which only require a limited number of further observations. The final use of the prediction models will be within process control. It is therefore assumed that parameter settings are looked for which lead to specific values of the properties temperature and velocity. It turns out that adjusting the GLMs with an additive constant leads to prediction results much closer to the observed values than the predicted values without the adjustment. As a final step two parameter settings are derived from the fitted adjusted model, which return predicted values close to the desired temperature and velocity of the particles. Verification experiments confirm these settings.

This paper is organized as follows. In Section 2 we introduce the experimental set-up for the thermal spraying process of interest. The measured in-flight properties are analysed in Section 3 and individual BIC-optimal GLMs are fitted. In Section 4 the day-adjustment strategy is presented and successfully applied to the prediction models for temperature and velocity. The paper finishes with an outlook and discussion in section 5.

2. Experimental set-up of the thermal spraying process

In this section, we give detailed information on the material and equipment used for the experiments.

The thermal spraying experiments were conducted with a Wokajet 400 HVOF spray gun from Sulzer. This gun is a liquid fuel gun using kerosene and pure gaseous oxygen for the combustion process. During all experiments an agglomerated and sintered WC-12Co powder of type WOKA 3102 from Sulzer Metco was used. Its chemical composition is given in Table 2.1. The particle size of $-45 + 15\mu m$ was determined by laser scattering and sieve analysis by Sulzer Metco Figure (2.1).

The powder was injected radial to the combustion gas flow directly behind the Laval nozzle by a TWIN 120AH powder supply. Acceleration nozzle length was

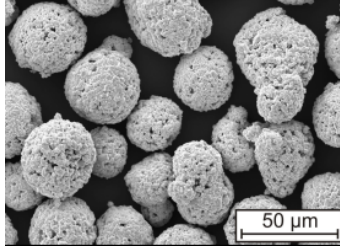| W	C	Co	Fe
82.3	5.48	12.13	0.09

Table 2.1: Powder chemical composition (wt.-%)

Figure 2.1: SEM-image of utilized WC-12Co powder from Sulzer Metco

kept constant at 6 inch and gun velocity (passing speed of gun over substrate) at 30m/min.

As substrate material 48.5×2.5mm steel tubes of 1.0503 mild steel were used for all experiments. To clean the surfaces and for better adhesion of the coatings, all tubes were grit blasted with Al_2O_3 (EKF 100) at a pressure of 4 bar from a distance of 100 mm at an angle of $45°$. Surface roughness R_z after grit blasting was $19 - 24\mu m$. One hour before spraying the specimens were cleaned in an ultrasonic ethanol bath for 30 min., dried and put into an electric furnace at $120°$C.

An Accuraspray g3 analyzing system from Tecnar was employed for particle velocity and temperature measurement. The particle sizes and shapes were recorded by an optical laser system of type VisiSizer N60 from Oxford Lasers. Both systems were mounted on a holder fixed to the spray cabin and synchronized to the same spot in the spray jet for each run. The measuring time in each run was marked by the VisiSizer system to count at least 300 particles.

3. Fitting of individual GLM

In this section we model the relationship between the process parameters and the individual in-flight properties separately as given in Figure 3.1. Previous analyses of the process (Hoyden, 2011) showed that fitting classical linear models does not lead to a good fit and that the assumption of a normal response distribution might not be valid. Hence we employ generalized linear models (GLMs) which allow the modeling of response variables $\mathbf{Y}$ which are assumed to follow a distribution from

Machine setting   In-flight properties

| Kerosine (K) |
| Stand-off-Distance (D) |
| Feeder Disc Velocity (FDV) |
| Lambda (L) |

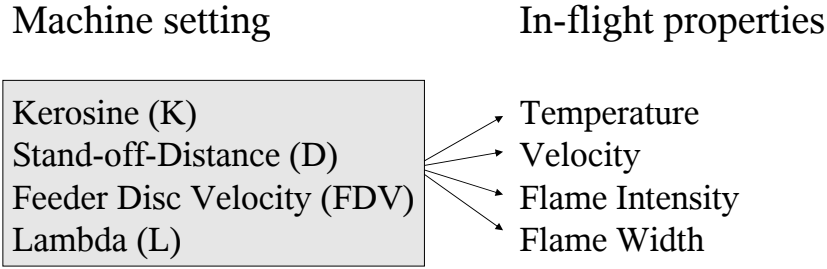Temperature
Velocity
Flame Intensity
Flame Width

Figure 3.1: List of parameters in the experimental set-up

a class within the exponential family. Let $E(\mathbf{Y})$ denote the expected value of the response variable $\mathbf{Y} \in \mathbb{R}^n$, which is expressed as

$$E(\mathbf{Y}) = \boldsymbol{\mu} = g^{-1}(\mathbf{X}\boldsymbol{\beta})$$

within the generalized linear model. Herein g is the so-called link function, where common choices are e.g. the inverse, the identity or the natural logarithm. The design matrix $\mathbf{X}$ contains observed values of the predictor variables. Apart from the process parameters themselves we can also consider squared effects and interaction terms as predictor variables.

As the final aim are sparse models with a good fit, the selection of predictor variables is an important issue. Two of the most popular variable selection criteria are the AIC (Akaike's Information Criterion, Akaike (1973)) and the BIC (Bayesian Information Criterion, Schwarz (1978)). A low value of the criteria indicates a good fit of the data. They are both based on the log-likelihood of the model and on the number of chosen predictor variables, but the BIC penalizes a high number of predictor variables stronger than the AIC. In different studies (consult Taper and Lele (2004) for an overview) it has been shown that BIC-optimal models are not as prone to overfitting as AIC-optimal models, so we choose the BIC as variable selection criterion.

Due to knowledge of the process we constrain the maximum number of predictors to nine. We denote p as the number of chosen variables, so that $\mathbf{X}$ is an $(n \times p)$-matrix. The unknown parameters $\boldsymbol{\beta}$ are commonly estimated by the maximum likelihood (ML) method. Then $\hat{\boldsymbol{\beta}}$ denotes the ML estimator. For further details we refer to

e.g. McCulloch and Searle (2001). One disadvantage of the information criteria is that they can be used only for comparisons of models for one and the same response variable. To judge the fit of a linear model and compare it to a completely different model, the coefficient of determination R^2 is a useful tool. Nagelkerke's coefficient of determination R_N^2 is an R^2-type criterion of fit for GLMs which can be interpreted as the explained ratio of variation in the data (Nagelkerke, 1991).

Residual analysis is a crucial part of (generalized) linear models. While quantile-quantile plots are considered in the case of classical linear models, we look at half-normal plots instead. Half-normal plots show the sorted absolute standardized residuals against the half normal quantiles ($\Phi^{-1}\left(\frac{n+i+\frac{1}{2}}{2n+\frac{9}{8}}\right)$) (McCullagh and Nelder, 1989), values strongly deviating from the dashed line are indicators for a unsuitable link function.

For the comparison of the different predictor subsets we use the statistical programming language R (R Development Core Team, 2011) and the package `bestglm` by McLeod and Xu (2010). After choosing the distribution, the link function and estimating the coefficients, we conduct residual analysis to check whether the assumptions of the GLM hold. Finally, we look at the R_N^2 computed with the package `pscl` by Jackman (2011).

Application to Real Data. An orthogonally blocked central composite design (CCD) has been chosen for the experimental design. A CCD consists of a full 2^k design (here: $k = 4$), center points and axial points, where one factor is set to $\alpha > 1$ (here: $\alpha = 2$ for orthogonally blocking) and the remaining ones are zero. With the CCD linear terms, quadratic terms and two-way interactions are estimable. The plan is given in Table A.1. The levels of the design are explained in Table 3.1. Instead of the oxygen level we use a kind of ration of the kerosine and oxygen level due to engineering reasons.

		Level			
Factor	-2	-1	0	1	2
Kerosene level (K)	15	17.5	20	22.5	25
Lambda (L)	1	1.075	1.15	1.225	1.3
Stand-off distance (D)	200	225	250	275	300
Feeder disc velocity (FDV)	5	7.5	10	12.5	15

Table 3.1: Parameter values

3. Fitting of individual GLM

For each of the four in-flight properties, temperature, velocity, flame intensity and flame width, generalized linear models with smallest BIC-values are determined. As predictor variables main effects, interaction as well as quadratic effects are allowed with the restriction of at most nine effects. With the logistic link, the identity link and the inverse link different link functions are compared whereas as response distribution the Gamma distribution turned out to be the most suitable assumption. If the half-normal plot of the BIC-minimal model suggests a pattern, we also consider the models with the next best fit. This is the case for velocity and flame width. We finally end up with the model with the second-best (for velocity) resp. third-best (for flame width) BIC.

Table 3.2 gives an overview of the selected models and their fit. The R_N^2 can be used to compare e.g. the chosen GLM for temperature and velocity but it mainly provides an idea of the quality of fit itself. In most cases (except for temperature) all possible main effects are included in the BIC-optimal model.

Finally we look at scatterplots of fitted values against residuals and fitted values against the index for a final check of the chosen model. Let us now look at the fitted models in more detail. We concentrate on the parameter estimates for the predictor variables, an intercept is included in every fitted GLM as well.

	Temperature	Velocity	Flame Width	Flame Intensity
Main effects	L, K, D	L, K, D, FDV	L, K, D, FDV	L, K, D, FDV
Squared effects	K^2	K^2	K^2	L^2, K^2, FDV^2
Interaction terms	$-$	$-$	$-$	$D \cdot FDV$
BIC	245.744	196.979	99.749	106.148
R_N^2	0.884	0.987	0.818	0.901
Link	identity	logistic	inverse	identity

Table 3.2: Properties of the chosen GLMs with Gamma-distributed response variable

The BIC-minimal model for temperature has five significant parameters (see Table 3.3). The kerosine level has a positive influence on the temperature, whereas the other three parameters have negative influences on it.

The left plot in figure 3.2 shows the half-normal plot. The observations are close to the dashed line which legitimates the choice of the link function. The two right side plots are the residual plots. They indicate that the fitted values are neither correlated to the residuals (middle), nor to the index (right). Plotting the residuals

	Estimate	Std. Error	t value	Pr(>|t|)
(Intercept)	1523.263	2.672	570.036	5.955e-53
L	-17.742	2.314	-7.669	5.035e-08
K	19.658	2.294	8.570	6.554e-09
D	-13.818	2.314	-5.973	3.092e-06
K^2	-9.990	2.081	-4.800	6.259e-05

Table 3.3: Best model for temperature with identity link function

against the input variables (A.1) also suggests no correlation. Hence we stay with the BIC-minimal model with identity link for the in-flight property temperature. The explained ratio of variance is about 88%, which is a satisfying result in this context.
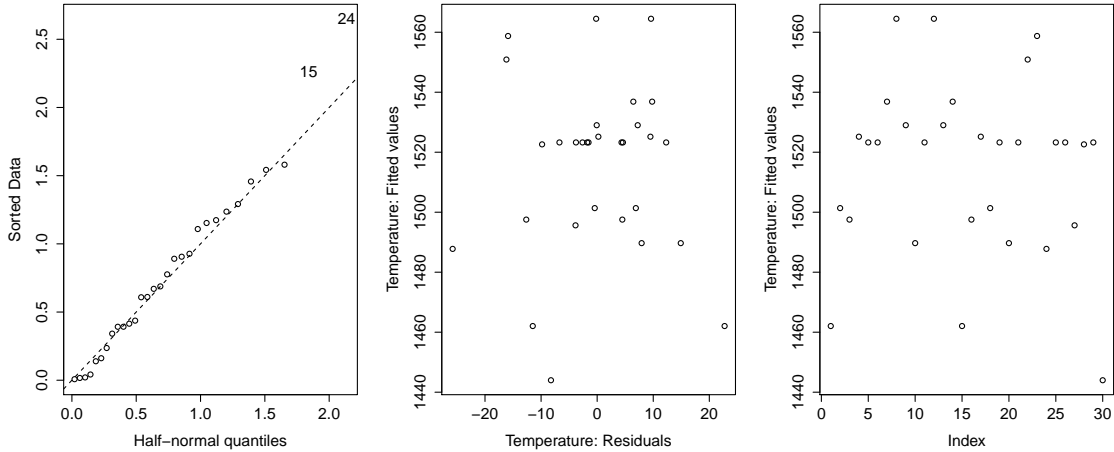

Figure 3.2: Temperature: Validation of assumptions of the GLM

The BIC-optimal model (BIC=195.178) for velocity shows irregularities in the half-normal plot, see Figure 3.3 (left). Therefore we investigate the properties of the model with the second-best BIC (BIC=196.979), which is a GLM with logistic link function. The corresponding half-normal plot is given on the right-hand side of Figure 3.3. We see no systematic differences between the dashed line and the observations, so in this case we take the GLM with logistic link function as final model. The best model for velocity (see Table 3.4) includes all linear predictors, plus the the interaction between L and K and the squared effect of K. The parameters are significant to the 5% level except for $L \cdot K$. Lambda and the kerosine level have positive effects on the velocity, the other parameters have negative effects on it.
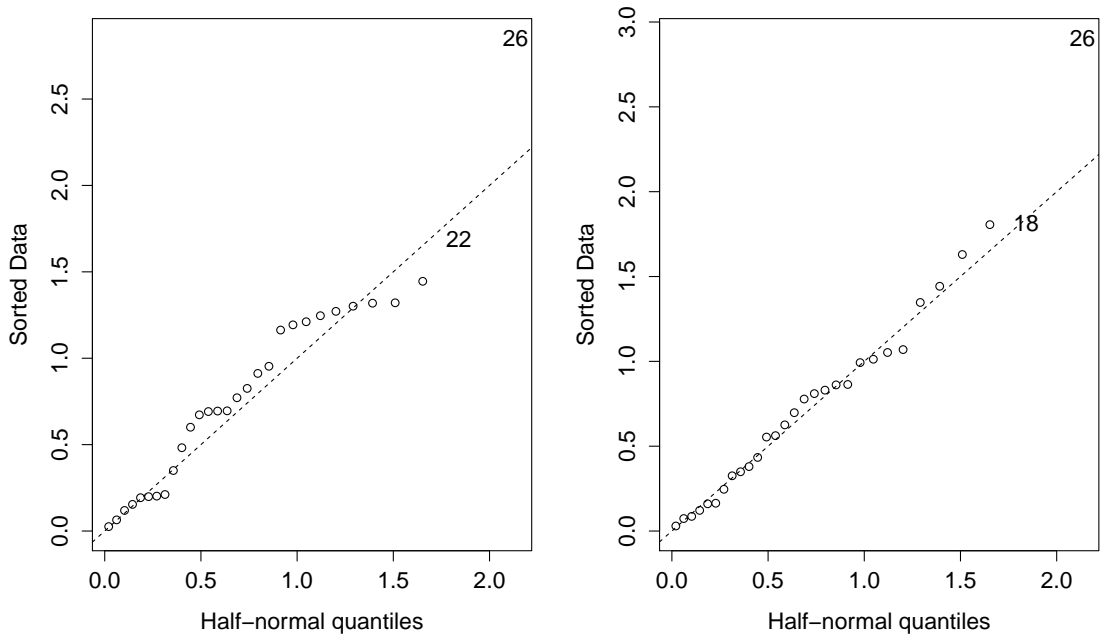
Figure 3.3: Half-normal plots of identity and logistic link function

	Estimate	Std. Error	t value	Pr($>$|t|)
(Intercept)	6.565e+00	1.564e-03	4198.393	3.510e-69
L	1.361e-02	1.354e-03	10.050	6.962e-10
K	5.161e-02	1.354e-03	38.112	2.732e-22
D	-1.711e-02	1.354e-03	-12.634	7.860e-12
FDV	-7.809e-03	1.354e-03	-5.767	7.112e-06
$L \cdot K$	-3.067e-03	1.659e-03	-1.849	7.733e-02
K^2	-9.169e-03	1.236e-03	-7.417	1.531e-07

Table 3.4: Best model for velocity with logistic link function

Further analysis (see Figure 3.4) shows no obvious violations against the assumptions of the GLM. Yet there is an interesting aspect in Figure A.2: Setting the input parameters zero seems to lead to smaller residuals. Nevertheless we stay with the BIC-minimal model with inverse link function.

The BIC-optimal model for flame width (BIC=87.390, identity link function) shows poor residual behaviour, such that the assumptions of model seem to be violated (see Figure 3.5, left). We observe the same for the second-best BIC (BIC=96.682, logistic link function, middle), which is why we consider a model with a slightly poorer BIC-value (BIC=99.748, inverse link function, right). These observations are much closer to the dashed line, so we decide on the GLM with inverse link
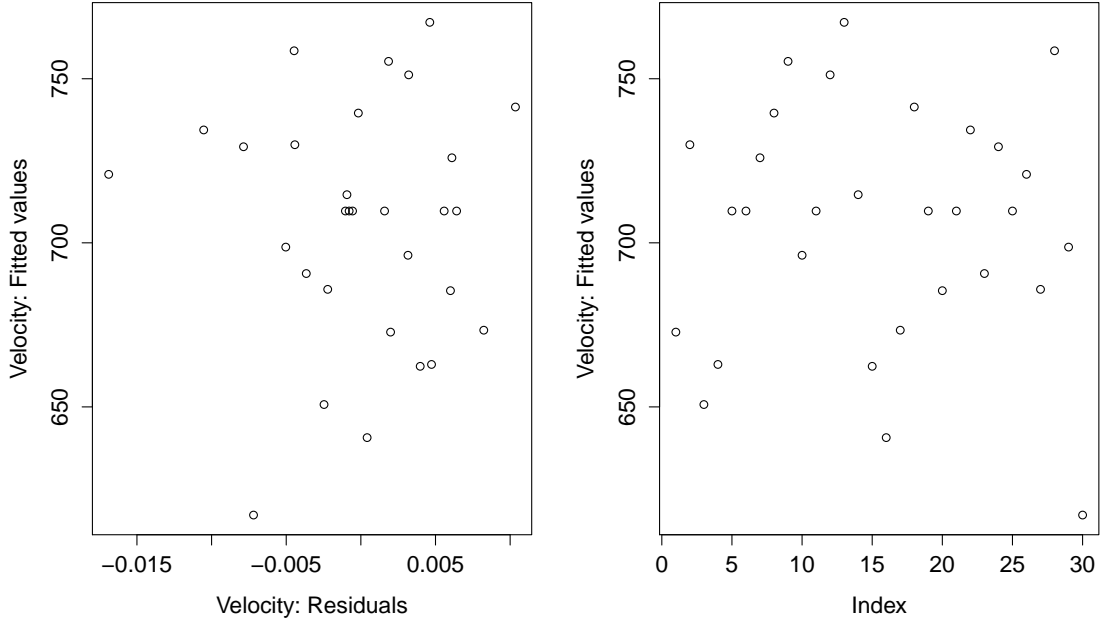
Figure 3.4: Velocity: Validation of assumptions of the GLM

function.

The GLM for flame width (see Table 3.5) is similar to that for velocity, except for the missing interaction between Lambda and Kerosin. Yet, there are notable differences. The stand-off-distance is not significant to the 5%-level, but we believe it is relevant in this model. Lambda, stand-off-distance and the squared kerosine level have positive effects on the flame width, the remaining parameters have negative effects.

	Estimate	Std. Error	t value	$\Pr(>|t|)$
(Intercept)	8.630e-02	1.808e-03	47.727	2.673e-25
L	5.296e-03	1.524e-03	3.476	1.956e-03
K	-4.439e-03	1.612e-03	-2.754	1.106e-02
D	2.867e-03	1.525e-03	1.880	7.236e-02
FDV	-1.231e-02	1.508e-03	-8.162	2.208e-08
K^2	3.904e-03	1.542e-03	2.532	1.832e-02

Table 3.5: Best model for flame width

The residual plots in Figure 3.6 and A.3 show no obvious violations of the model assumptions. Hence, we chose the model with inverse link and predictor variables as given in Table 3.5.
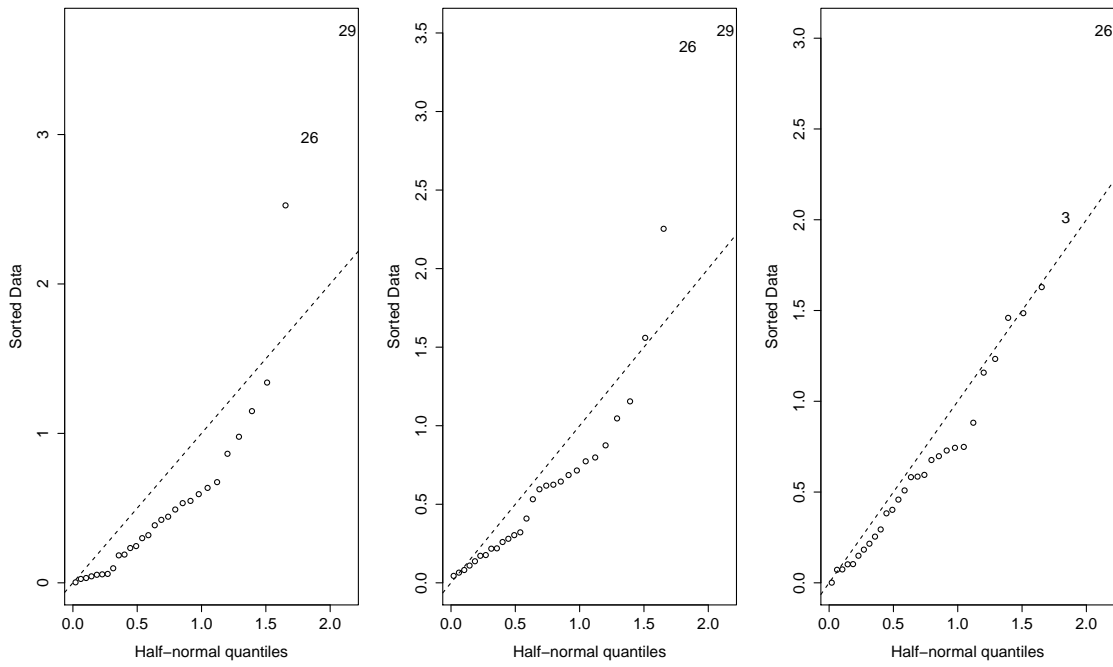
11

Figure 3.5: Half-normal plots for GLMs with identity, logistic and inverse link function (f.l.t.r.)
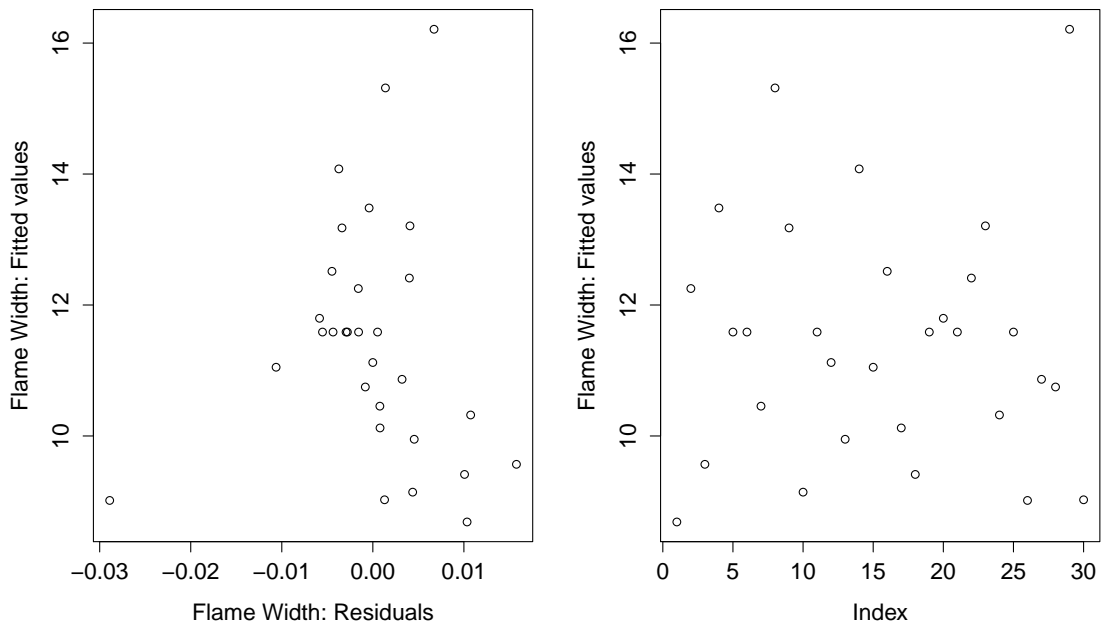

Figure 3.6: Flame Width: Validation of assumptions of the GLM

The model with the most parameters is the best model for flame intensity (Table 3.6). There are non-significant parameters (stand-off-distance, squared Lambda, interaction between stand-off-distance and feeder disc velocity), but we do not rely on the p-value only. We have four positive effects on the flame intensity and four negative effects. The assumptions of the GLM seem to hold, since there are no obvious patterns in Figures 3.7, A.4 and A.5.

	Estimate	Std. Error	t value	Pr($>$|t|)
(Intercept)	19.478	0.336	57.905	1.188e-24
L	-0.889	0.190	-4.675	1.296e-04
K	0.865	0.186	4.641	1.405e-04
D	-0.371	0.197	-1.883	7.360e-02
FDV	2.166	0.204	10.606	6.851e-10
L^2	-0.310	0.176	-1.759	9.311e-02
K^2	-0.561	0.170	-3.306	3.365e-03
FDV^2	0.509	0.192	2.646	1.512e-02
$D \cdot FDV$	0.410	0.238	1.722	9.976e-02

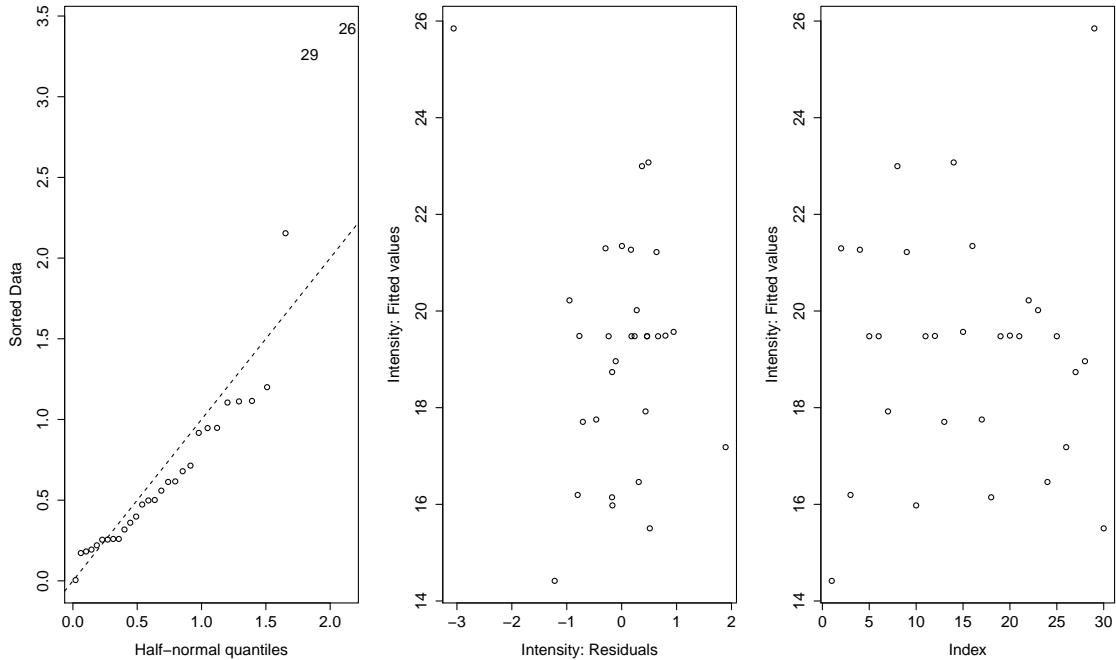Table 3.6: Best model for flame intensity

Figure 3.7: Flame Intensity: Validation of assumptions of the GLM

In conclusion, we remark that the kerosine level and the squared kerosine level are contained in each of the final GLMs, but with different signs in different models.
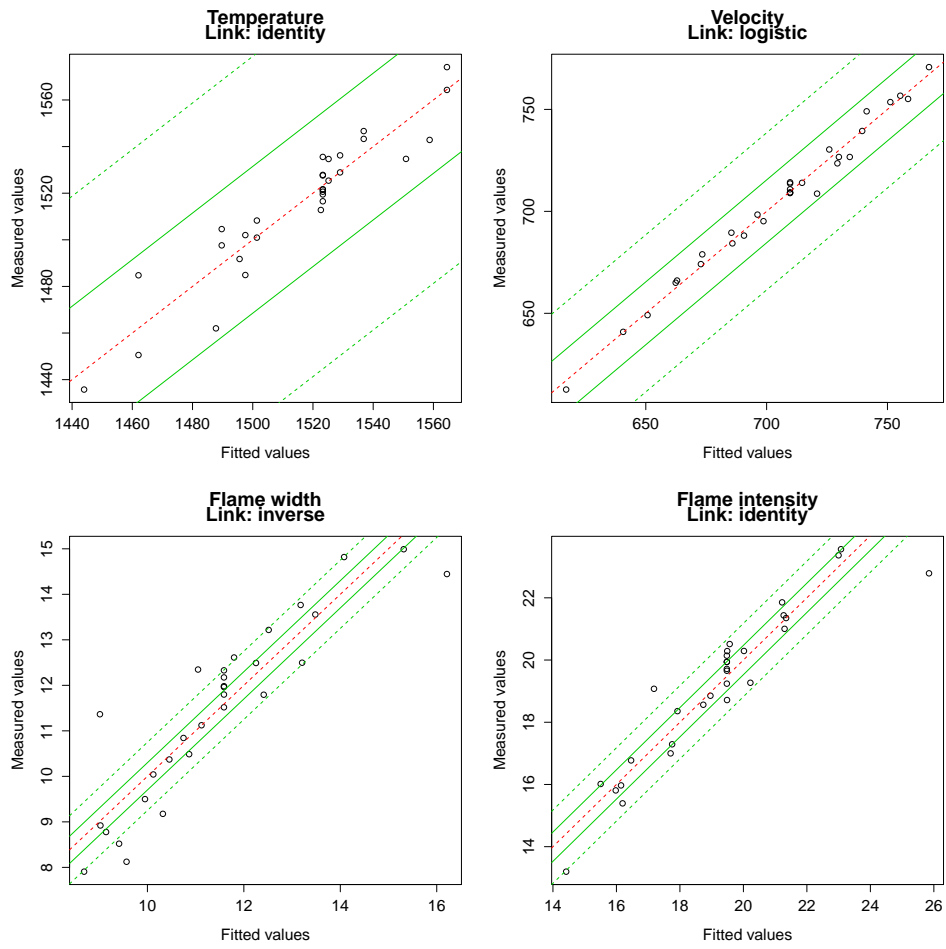
Figure 3.8: Prediction quality of the properties in flight

Finally, in Figure 3.8, the estimated values are plotted against the observed ones for the chosen models. Points which are located on the red dashed line are perfect predictions of the true values, points between the green solid lines are predictions with less than 2% inaccuracy. Points between the green dashed lines are predictions with less than 5% inaccuracy. We see that the predictions of temperature and velocity are less than 2% inaccurate. The predictions of the flame properties are mostly less than 5% inaccurate.

4. Day-adjusted prediction of coating properties

We now describe our procedure to adapt generalized linear models from a more extensive preceding study, such as the final models from the previous section, to additive day-effects by using only a limited number of new experiments on the prediction day. In our application to thermal spraying our final goal are parameter settings which lead to desired values of 1550 for the temperature and 740 for velocity. Let $X_1 \in \mathbb{R}^{n \times k}$ be the design matrix from the preceding study, here the central composite design given in Table A.1, and

$$g(\mu) = \eta_1 = X_1 \beta_1,$$

the considered generalized linear model with appropriately chosen link function g. The corresponding maximum likelihood estimation $\hat{\beta}_1$ is the basis for the subsequent day-adjustment. In order to adapt the model to another day we estimate an additive constant based on a design X_2, conducted on the day of interest, here a fractional factorial with 8 runs in total, in the following sense

$$\eta_2 = X_2 \hat{\beta}_1 + \gamma,$$

where a constant $\gamma \in \mathbb{R}$ is added to the linear predictor. The additive term γ is estimated by the maximum likelihood method based on the observed data from conducting the experiments from the design X_2. This leads us to the following new prediction model

$$\hat{y} = g^{-1} \left(X \hat{\beta}_1 + \hat{\gamma} \right),$$

where g^{-1} is the inverse map of the link function belonging to the original GLM. For our particle properties temperature and velocity the resulting adapted models are

$$\hat{y}_T = g_T^{-1} \left(X \hat{\beta}_T + \hat{\gamma}_T \right) \text{ and}$$
$$\hat{y}_V = g_V^{-1} \left(X \hat{\beta}_V + \hat{\gamma}_V \right),$$

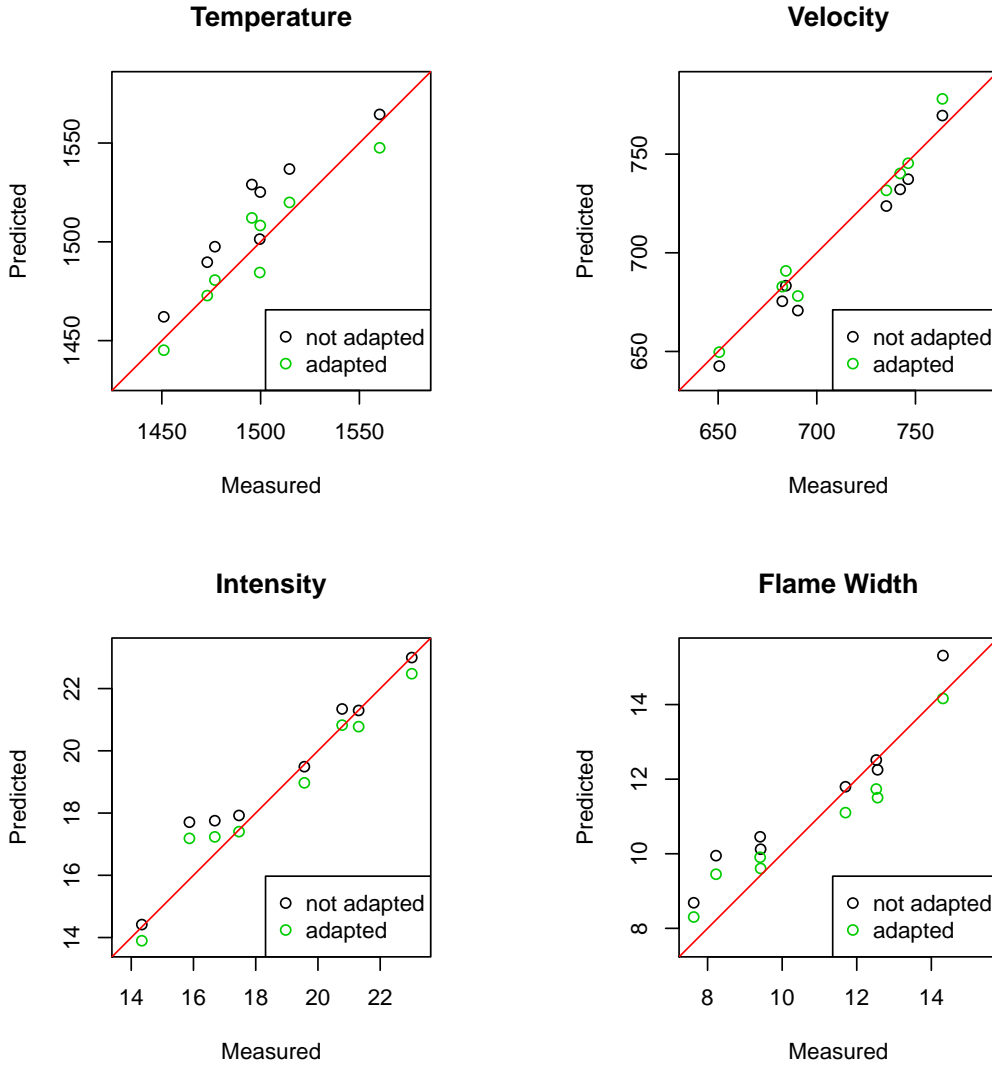with g_T^{-1} the identity, g_V^{-1} the exponential function and estimates as given in Table A.2.

Figure 4.1: Real vs. Fitted for adapted and original models for temperature, velocity, flame width and intensity

Figure 4.1 shows the measured values for temperature and velocity versus the fitted values. It is rather obvious that a model adaption is necessary, especially for the temperature. With the additional constant, the root mean squared error reduces from 388.444 to 101.220 for temperature and from 98.768 to 49.473 for velocity. Hence, even for the simple modification by a single additive constant we have substantially improved the prediction model.

Based on the day-adjusted models parameter settings are searched for which lead to predicted particle property values close to the desired ones. To achieve this for both

temperature and velocity simultaneously as best as possible, the Joint Optimization Plot method (Erdbrügge *et al.*, 2011) has been used. It returns points on the Pareto front. Two possible parameter settings were chosen and verified by two experiments each. The results are rather convincing, as predicted and observed values are very close, see Table 4.1.

L	K	SOD	FDV	Temperature		Velocity	
				Predicted	Observed	Predicted	Observed
-1.28	0.51	-1.15	- 0.64	1549.21	1551.48	739.90	743.19
-1.28	0.51	-1.15	- 0.64	1549.21	1556.17	739.90	742.81
-0.23	0.48	-1.44	1.24	1549.93	1552.97	739.96	742.60
-0.23	0.48	-1.44	1.24	1549.93	1521.02	739.96	723.82

Table 4.1: Results of prediction and verification experiments

5. Outlook and Discussion

The overall idea of our research is the assumption that the particle properties reflect some non-controllable disturbances of the thermal spraying process, like a day effect. Thereby it should be possible to gain better predictions of the coating properties on the basis of the particle properties. As a first step, we have here modeled the particle properties by means of generalized linear models and were able to find parameter settings which lead to desired temperature and velocity values. Some further improvements with respect to modeling in-flight properties might be achieved by considering generalized additive models, where some regressors can be treated more exactly. Future research will focus on strategies for predicting the coating properties. To this aim models for particle and coating properties are connected. The results will be presented in a forthcoming discussion paper.

This paper discusses the spraying process when WC-Co layers are used. These kinds of layers have possible negative effects on health, which is why these (and other) investigations will be extended to iron-based layers. The exact chemical composition of such an iron-based layer is a recent field of research and investigations of the spraying process as in section 3 but with iron-based layers promises to be a highly interesting topic.

Acknowledgements

References

Akaike H (1973). "Information Theory and an Extension of the Maximum Likelihood Principle." *Proceedings of the Second International Symposium on Information Theory.*

Erdbrügge M, Kuhnt S, Rudak N (2011). "Joint optimization of independent multiple responses." *Quality and Reliability Engineering International,* **27**(5), 689–703. ISSN 07488017. doi: 10.1002/qre.1229.

Hoyden L (2011). "Wahl einer geeigneten Linkfunktion im generalisierten linearen Modell mit Anwendung auf einen thermokinetischen Spritzprozess." *Bachelor thesis,* TU Dortmund University.

Jackman S (2011). "pscl: Classes and Methods for R Developed in the Political Science Computational Laboratory, Stanford University." URL `http://pscl.stanford.edu/`.

McCullagh P, Nelder JA (1989). *Generalized Linear Models.* Chapman & Hall, London.

McCulloch CE, Searle SR (2001). *Generalized, linear, and mixed models.* John Wiley & Sons, New York. ISBN 047119364X.

McLeod A, Xu C (2010). "bestglm: Best Subset GLM." URL `http://CRAN.R-project.org/package=bestglm`.

Nagelkerke NJD (1991). "A note on a general definition of the coefficient of determination." *Biometrika,* **78**(3), 691–692. ISSN 0006-3444. URL `http://www.jstor.org/stable/2337038?origin=crossref`.

R Development Core Team (2011). *R: A Language and Environment for Statistical Computing.* R Foundation for Statistical Computing, Vienna, Austria. ISBN 3-900051-07-0, URL `http://www.R-project.org/`.

Schwarz G (1978). "Estimating the Dimension of a Model." *The Annals of Statistics,* **6**(2), 461–464. ISSN 0090-5364.

References

Taper ML, Lele S (2004). *The nature of scientific evidence: statistical, philosophical, and empirical considerations.* University of Chicago Press, Chicago.

Tillmann W, Vogli E, Hussong B, Kuhnt S, Rudak N (eds.) (2010). *Relations between in flight Particle Characteristics and Coating Properties by HVOF Spraying,* volume 264. DVS-Berichte. ISBN 978-3-87155-590-9.

A. Appendix

Run	L	K	D	FDV
1	1	-1	1	-1
2	1	1	1	1
3	-1	-1	1	-1
4	-1	-1	-1	1
5	0	0	0	0
6	0	0	0	0
7	-1	1	1	-1
8	-1	1	-1	1
9	1	1	-1	1
10	1	-1	-1	-1
11	0	0	0	0
12	-1	1	-1	-1
13	1	1	-1	-1
14	-1	1	1	1
15	1	-1	1	1
16	-1	-1	1	1
17	-1	-1	-1	-1
18	1	1	1	-1
19	0	0	0	0
20	1	-1	-1	1
21	0	0	0	0
22	0	0	-2	0
23	-2	0	0	0
24	2	0	0	0
25	0	0	0	0
26	0	0	0	-2
27	0	0	2	0
28	0	2	0	0
29	0	0	0	2
30	0	-2	0	0

Table A.1: Central Composite Design

A. Appendix

	$\hat{\beta}_T$	$\hat{\beta}_V$
(Intercept)	1523.263	6.565
L	-17.742	0.014
K	19.658	0.052
D	-13.818	-0.017
FDV		-0.008
K^2	-9.990	-0.009
$L \cdot K$		-0.003
$\hat{\gamma}$	-16.897	0.0109

Table A.2: Estimators for β and γ
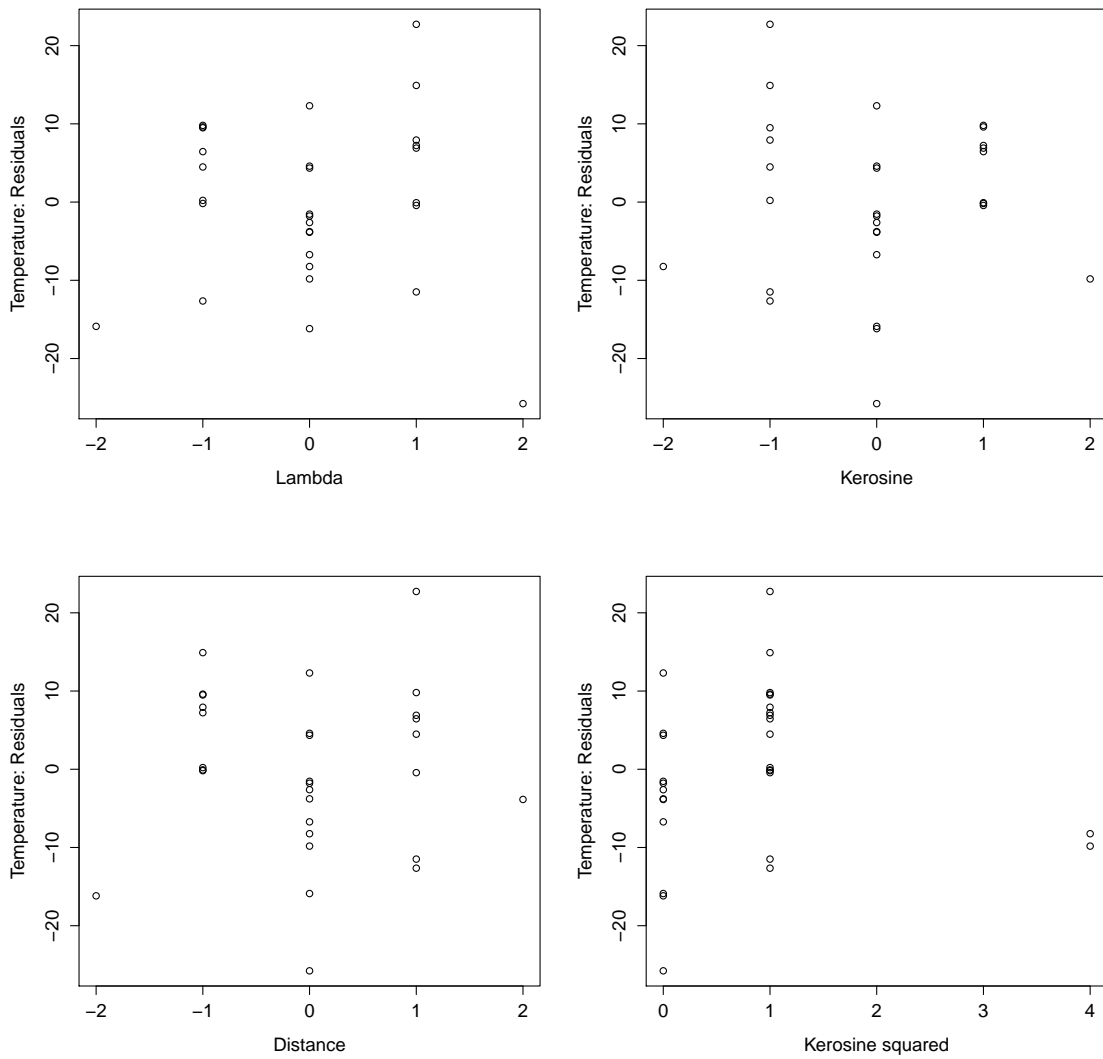
Figure A.1: Temperature: Further residual analysis of the GLM
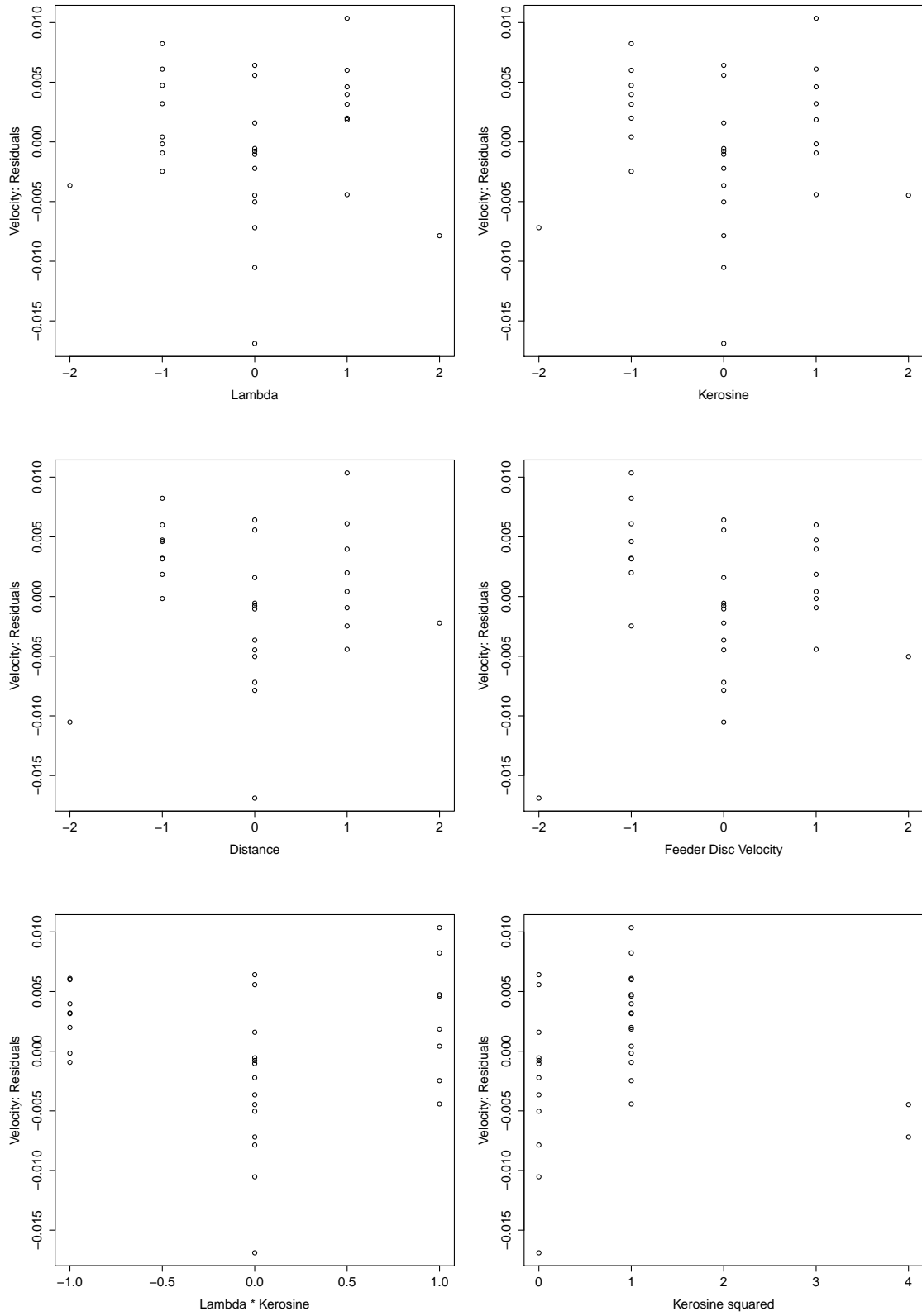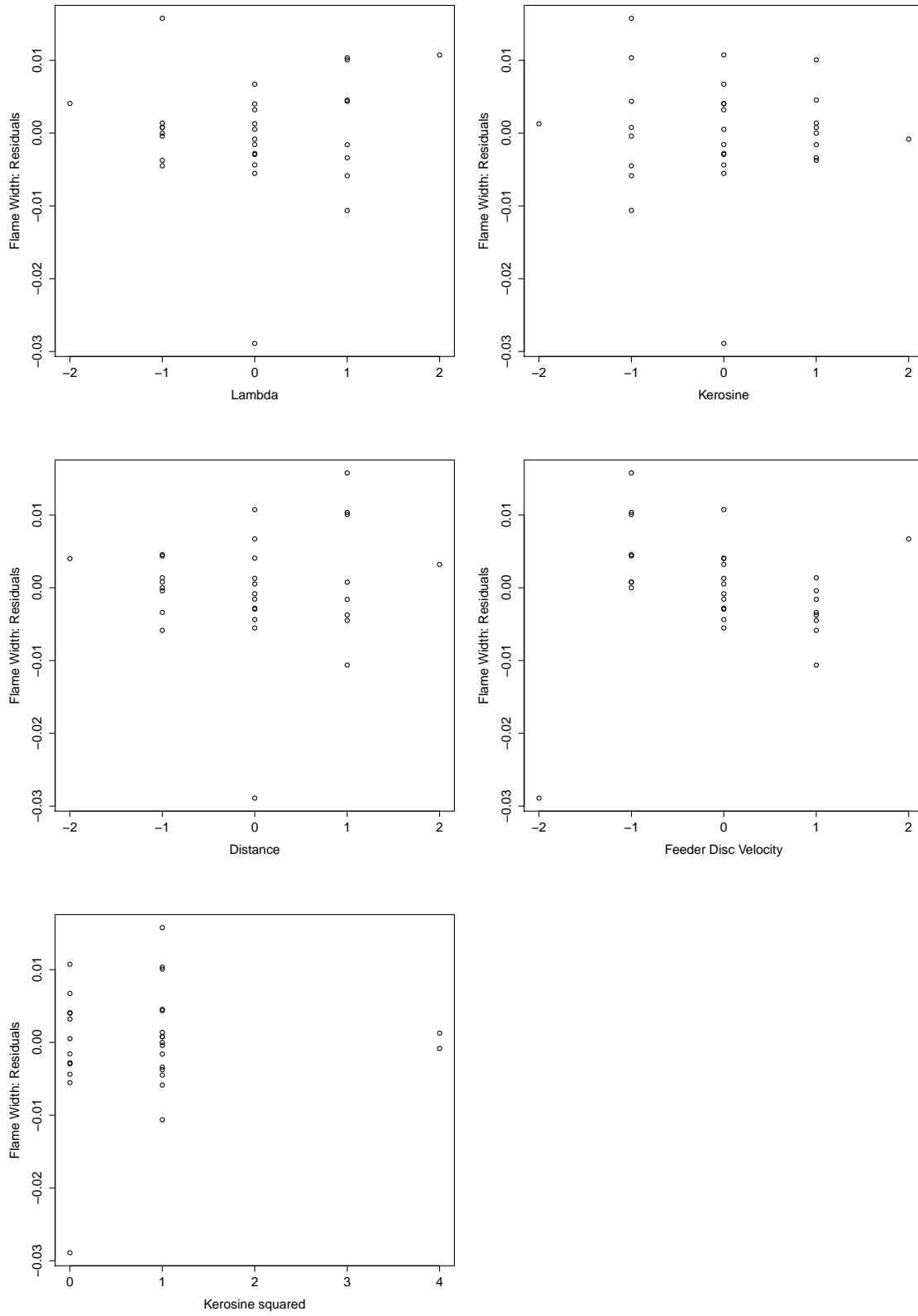
Figure A.2: Velocity: Further residual analysis of the GLM
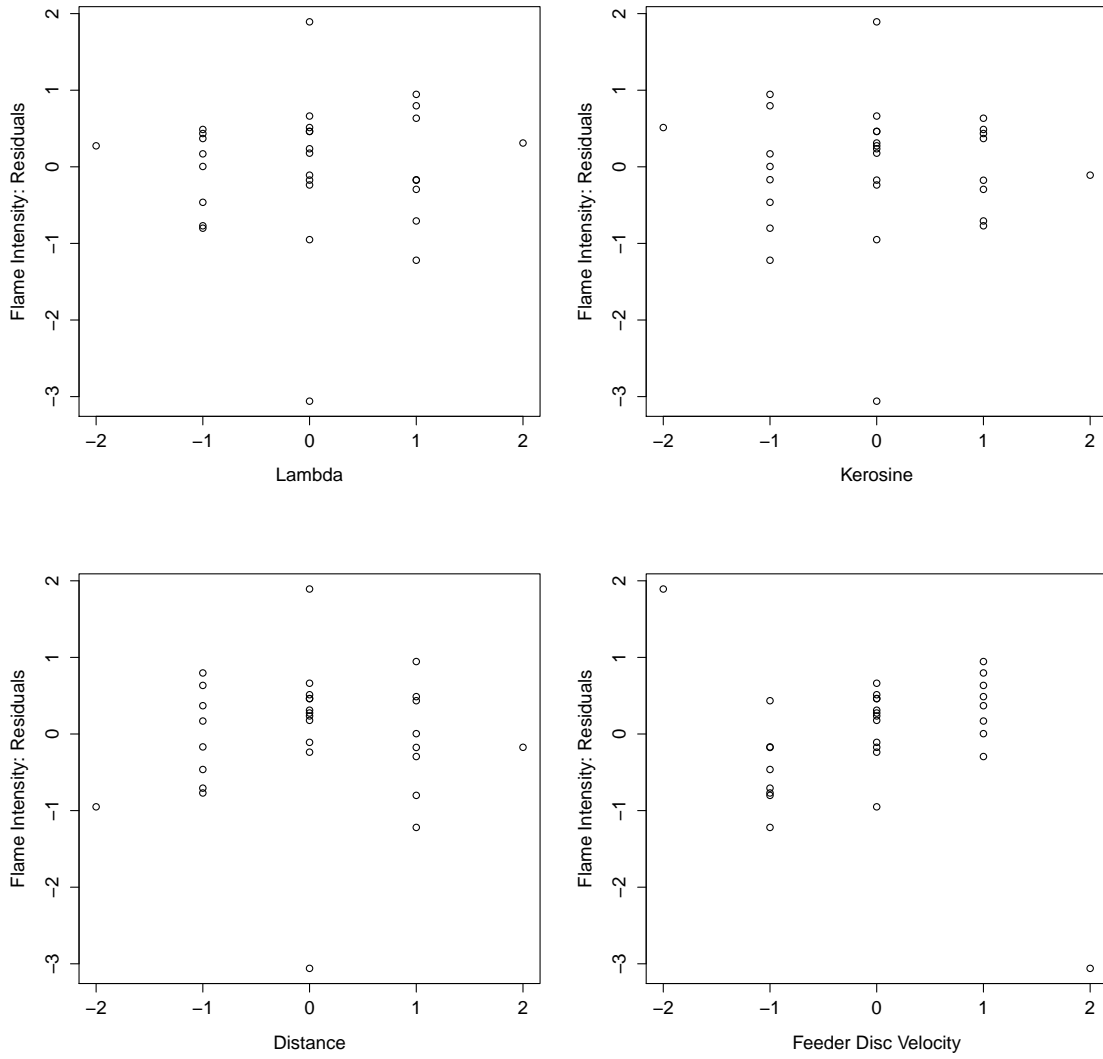
Figure A.3: Flame Width: Further residual analysis of the GLM

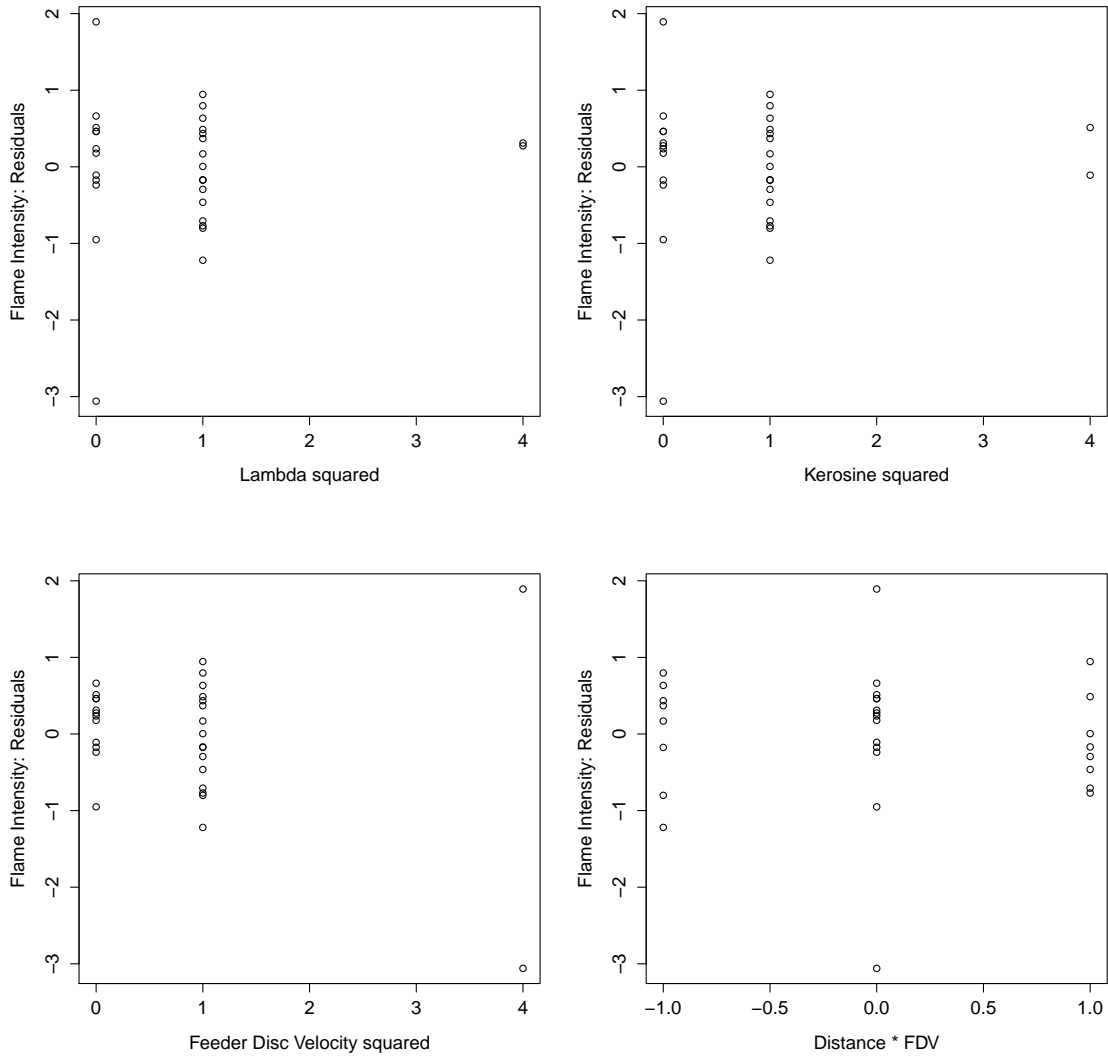Figure A.4: Flame Intensity: Further residual analysis of the GLM (main effects)

Figure A.5: Flame Intensity: Further residual analysis of the GLM (other effects)

Run	L	K	D	FDV
1	1	1	-1	-1
2	1	-1	-1	1
3	-1	-1	-1	-1
4	-1	-1	1	1
5	-1	1	1	-1
6	1	1	1	1
7	1	-1	1	-1
8	-1	1	-1	1

Table A.3: The reduced design for X_2